

Geoheritage

Natural laboratories for field observation about genesis and landscape effects of palaeo-earthquakes: a proposal for the Rocca Busambra and Monte Barracù geosites (W Sicily) --Manuscript Draft--

| | |
|--|---|
| Manuscript Number: | GEOH-D-17-00080R2 |
| Full Title: | Natural laboratories for field observation about genesis and landscape effects of palaeo-earthquakes: a proposal for the Rocca Busambra and Monte Barracù geosites (W Sicily) |
| Article Type: | Original Article |
| Corresponding Author: | Luca Basilone Universita degli Studi di Palermo Dipartimento di Scienze della Terra e del Mare ITALY |
| Corresponding Author Secondary Information: | |
| Corresponding Author's Institution: | Universita degli Studi di Palermo Dipartimento di Scienze della Terra e del Mare |
| Corresponding Author's Secondary Institution: | |
| First Author: | Luca Basilone |
| First Author Secondary Information: | |
| Order of Authors: | Luca Basilone Alessandro Bonfardeci Pierangelo Romano Attilio Sulli |
| Order of Authors Secondary Information: | |
| Funding Information: | |
| Abstract: | <p>Earthquakes are phenomena that are still being learned by the scientific community, and poorly known, especially as regard the prevention, by the population. Having a more complete knowledge is a basic step in understanding the vastness and intensity of the destructive phenomenon that involves a great amount of people. The recent earthquakes occurred in Central Italy (L'Aquila and Amatrice earthquakes) are examples that demonstrate the importance of having knowledge about these phenomena to contrast their destructive effects.</p> <p>We present a geological field trip to recognise causes and landscape effects of palaeo-earthquakes recorded in the Mesozoic rock successions outcropping in Sicily. The isolated carbonate reliefs of Rocca Busambra and Monte Barracù (Sicani Mts.) are spectacular sites of a passive continental margin where synsedimentary tectonic features – as paleofaults, neptunian dykes, morphostructural scarps, submarine landslide, soft sedimentary deformation structures – document earthquake causes and effects. Field evidence show in detail as the several paleofaults mapped in the Rocca Busambra stepped margin triggered the soft-sediment deformation structures recorded in the coeval deep-water rock succession of the Monte Barracù.</p> <p>In this view, the proposed field trip can represent a powerful tool to enhance the naturalistic and geological importance of the study areas by establishing geosites and protected areas for a proper fruition of geological-natural heritage and/or for geoconservation. Thus, through the proposed field trip it is possible to observe paleo-earthquakes activity and landscape products, having an educational training purpose also for public administrators, whose rapid and skilled action is necessary for the prevention and reduction of the geohazard.</p> |
| Response to Reviewers: | we have accepted all the suggestions of the reviewer |

[Click here to view linked References](#)

1 **Natural laboratories for field observation about genesis and landscape effects of palaeo-**
2 **earthquakes: a proposal for the Rocca Busambra and Monte Barracù geosites (W Sicily)**

3
4
5 3
6
7 4 Luca Basilone*, Alessandro Bonfardeci, Pierangelo Romano, Attilio Sulli

8
9 5
10
11
12 6 *Department of Earth and Marine Science, University of Palermo, Via Archirafi 22, 90123*

13
14 7 *Palermo, Italy*

15
16 8
17
18
19 9 *corresponding author: luca.basilone@unipa.it

20
21 10
22
23
24
25
26
27
28
29
30
31
32
33
34
35
36
37
38
39
40
41
42
43
44
45
46
47
48
49
50
51
52
53
54
55
56
57
58
59
60
61
62
63
64
65

11 **Abstract**

1
2 12 Earthquakes are phenomena that are still being learned by the scientific community, and
3
4 13 poorly known, especially as regard the prevention, by the population. Having a more complete
5
6 14 knowledge is a basic step in understanding the vastness and intensity of the destructive
7
8 15 phenomenon that involves a great amount of people. The recent earthquakes occurred in Central
9
10
11
12 16 Italy (L'Aquila and Amatrice earthquakes) are examples that demonstrate the importance of
13
14 17 having knowledge about these phenomena to contrast their destructive effects.

16 18 We present a geological field trip to recognise causes and landscape effects of palaeo-
17
18
19 19 earthquakes recorded in the Mesozoic rock successions outcropping in Sicily. The isolated
20
21
22 20 carbonate reliefs of Rocca Busambra and Monte Barracù (Sicani Mts.) are spectacular sites of
23
24 21 a passive continental margin where synsedimentary tectonic features – as paleofaults, neptunian
25
26 22 dykes, morphostructural scarps, submarine landslide, soft sedimentary deformation structures
27
28
29 23 – document earthquake causes and effects. Field evidence show in detail as the several
30
31 24 paleofaults mapped in the Rocca Busambra stepped margin triggered the soft-sediment
32
33
34 25 deformation structures recorded in the coeval deep-water rock succession of the Monte Barracù.

36 26 In this view, the proposed field trip can represent a powerful tool to enhance the naturalistic
37
38
39 27 and geological importance of the study areas by establishing geosites and protected areas for a
40
41 28 proper fruition of geological-natural heritage and/or for geoconservation. Thus, through the
42
43
44 29 proposed field trip it is possible to observe paleo-earthquakes activity and landscape products,
45
46 30 having an educational training purpose also for public administrators, whose rapid and skilled
47
48
49 31 action is necessary for the prevention and reduction of the geohazard.

50
51 32
52
53 33 *Keywords:* geotourism; geoconservation; earthquake; synsedimentary faults; seismogenic
54
55 34 slumps; field trip
56
57
58
59
60
61
62
63
64
65

1. Introduction

An earthquake is ‘the shaking of the surface of the Earth, resulting from the sudden release of energy in the Earth's crust or upper mantle usually caused by movement along a fault plane and resulting in the generation of seismic waves, which can be destructive’ (Bolt 1993; Moczo et al. 2014). Earthquakes can trigger landslides, occasionally volcanic activity and, if located offshore, they can displace the seabed sufficiently to cause a tsunami (Keefer 2002; Malamud 2004; Walter and Amelung 2007; Posamentier and Martinsen 2011; Nishimura 2017).

Seismites are very important geological structures representing the evidence of the effects of earthquake in the sedimentary records (Seilacher 1969). These deformational structures, formed during seismic events of various values of magnitude, interested unconsolidated sediments. They also provide information about the responsible faults and the frequency of the earthquakes in a particular geological region (Seth et al. 1990; Mastalerz and Wojewoda 1993; Martinez et al. 2005; Gamboa et al. 2010; Strasser et al. 2011; Festa et al. 2014; Üner et al. 2017). Seismically-induced slides and slumps related to low-angle slope irregularities at the water–sediment interface have been reported from deep-water carbonates (Garcia-Tortosa et al. 2011; Mastrogiacomo et al. 2012; Bergerat et al. 2011; Ortner and Kilian 2016; Basilone et al. 2014, 2016a). By the way, other triggering mechanisms (e.g., storm waves, floods, overpressure, gravitational instability, tidal shear), which are “virtually” dependent of the depositional environment, may lead to sediment deformation structures (e.g., Owen et al. 2011; Van Loon and Pisarska-Jamroży 2014; Kopf et al. 2016; Lunina and Gladkov 2016).

Rocca Busambra (1613 m a.s.l.) and Monte Barracù (1420 m a.s.l.) are isolated carbonate reliefs, located in the W Sicani Mountains near Corleone (Palermo, Figs. 1a, 2a), representing an ancient passive margin (i.e. the Southern Tethyan continental margin) where causes and effects of possible Mesozoic earthquakes are observable. They consist in neptunian dykes, paleofaults, unconformities and soft-sediment deformation structures (SSDSs) which are

60 possible effects of synsedimentary tectonics and that could give information about the
61 occurrence of earthquake shocks and their intensity (Allen 1986; Obermeier 1996; Bourrouilh
62 1998; Leeder 2010; Alsop et al. 2016).

63 Neptunian dykes are enlarged fractures of lithified deposits that are subsequently filled by
64 younger sediment. Rocca Argenteria, the westernmost sector of the Rocca Busambra ridge
65 (Figs. 2a, b), is an excellent site to observe these features. Here, the several neptunian dykes
66 cutting the Lower Jurassic peritidal limestone are filled by different generation of sediments
67 that record the effect of a polyphased extensional tectonics (Wendt 1965, 2017; Martire and
68 Montagnino 2002; Basilone 2009).

69 Paleofaults are recognizable when angular unconformity between faulted beds and
70 undeformed younger deposits occur (Davies and Reynolds 1996; Miall 2016). Rocca
71 Busambra, especially the Piano Pilato region (Figs. 2a, b), includes spectacular sites where
72 morphostructural scarps and paleofaults draped by younger sediments are observable.

73 SSDSs record sedimentary and tectonic processes in various geological provinces. They
74 develop when primary lamination and stratification is deformed by a system of driving forces,
75 such as gravitational instability, during/after sedimentation and before complete lithification
76 (Allen 1986; Leeder 1987). Among the various SSDSs, those induced by earthquakes, initially
77 called seismites by Seilacher (1969), are common in different depositional environments, when
78 the sediment is temporarily in a weakened state due to the action of a deformation mechanism,
79 such as liquefaction and fluidization (Lowe 1976; Maltman 1984; Martinsen 1994; Owen and
80 Moretti 2011; Moretti et al. 2016). At Monte Barracù, SSDSs related to tectonic events and
81 attributed to earthquake shocks are well represented (Figs. 2a, c, Basilone 2017).

82 The main purpose of this work, which describes the results of detailed field investigation
83 and new data about the outcropping Mesozoic carbonates, is to give new information about the
84 geological heritage of the region. This approach allows us to emphasize the scientific and

85 geotouristic attraction of those features indicating the occurrence of synsedimentary tectonics
86 and the landscape effects of paleo-earthquakes.

87 Recent researches, highlighting geological, geomorphologic, naturalistic and cultural
88 heritages of Rocca Busambra region (e.g., the Royal Palace of Ficuzza, the hunting lodge of
89 Ferdinand III of the Kingdom of Sicily, since the 1799) and Monte Barracù ([Mascle 1979](#);
90 [Agate et al. 1998](#); [Basilone 2009](#); [2011](#); [Bertok and Martire 2009](#); [Catalano et al. 2010](#); [2011](#)),
91 are adequate to justify the proposition of Geosite for the areas. As indicated by the IUGS
92 (International Union of Geological Science) and by the UNESCO, a geosite is a place
93 characterised by relevant naturalistic features that should be preserved as geological heritage
94 ([Wimbledon 1997](#)). Geoconservation is an activity of importance to all geologists: it is a vital
95 support to the prosecution of geological research, education and training ([ProGEO 2011](#)). In
96 this view, the present paper should be used as a field trip guide for the observation and study of
97 the main characteristics related to the occurrence of earthquakes. It aims to the development of
98 economic and touristic interests with the proposition of geological itineraries for geotourism
99 (e.g., [Strasser et al. 1995](#); [Eder and Patzak 2004](#); [Basilone and Di Maggio 2016](#)).

101 2. Geological setting

102 The Sicilian orogen, located in the centre of the Mediterranean at the NE corner of the
103 Pelagian platform of North Africa, links the Southern Apennine and the Calabrian Arc to the
104 Tellian and Atlas systems (inset in Fig. 1a). The Sicilian Fold and Thrust Belt (FTB) is a
105 segment of the Apennine-Tyrrhenian System ([Amodio-Morelli et al. 1976](#); [Grandjacquet and](#)
106 [Mascle 1978](#); [Bigi et al 1990](#); [Vai and Martini 2001](#)), whose up-build is referred both to the
107 post-collisional convergence between Africa and a complex “European” crust and the coeval
108 roll-back of the subduction hinge of the Adriatic Ionian-African lithosphere ([Malinverno and](#)
109 [Ryan 1986](#); [Kastens et al. 1988](#)). The Sicilian FTB originates from the piling-up of tectonic

110 bodies, underway since the Miocene, deriving from the deformation of the paleogeographic
111 domains developed during the Mesozoic in the Southern Tethyan rifted continental margin. In
112 western Sicily the geometry of the thick-skinned accretionary wedge, as shown by geological
113 mapping (Broquet 1968; Mascle 1979; Catalano et al. 2010; 2011; Basilone 2011) and by
114 several regional seismic profiles (Catalano et al. 1998, 2008), displays a pile of thrust sheets
115 formed by different structural elements separated by S- and SW-vergent regional thrusts (Figs.
116 1a, b) and accompanied by clockwise rotation of the allocthonous sheets (Oldow et al. 1990).
117 They are characterized by: i) imbricated thrust wedge of Meso-Cenozoic shallow-water
118 carbonate units, up to 10 km thick (Trapanese tectonic units); ii) up to 3 km-thick mostly flat-
119 lying Meso-Cenozoic deep-water carbonate units (Sicanian units), overthrusting the deformed
120 carbonate platform rock units; iii) thin nappes of Cretaceous to Neogene deep-water (oceanic)
121 deposits of the Sicilide domain (Ogniben 1960) and Numidian flysch, detached from their
122 mainly carbonate substrate. The upper Miocene to Lower Pleistocene clastics, carbonates and
123 evaporites unconformably seal the underlying shortened tectonic units, filling wedge-top basins
124 (Broquet et al. 1984; Roure et al. 1990; Gasparo Morticelli et al., 2015). The Pleistocene-
125 Holocene continental and marine deposits (Di Maggio et al. 2009; Agate et al. 2017), frequently
126 mask the original tectonic contacts.

2.1. Study area

129 The study area (Fig. 1a) is comprised in the Sicanian thrust system, where the imbrication
130 has repeatedly involved the whole Sicanian succession (Mascle 1970, 1979; Roure et al. 1990;
131 Catalano et al. 1998; Monaco et al. 2000). In this tectonic frame, the Rocca Busambra tectonic
132 unit extends for about 15 km with an E–W-trending large antiform slightly rotated to the NW–
133 SE on its eastern side (Pizzo Marabito). The structure is bounded by two E–W major reverse
134 faults, with right-handed strike-slip movements (Fig. 1a). The Barracù ridge, consisting of two

135 main adjacent morphological culminations, is an arcuate structure formed by the emplacement
136 of two tectonic units along a low-angle thrust, displaying inside the typical characteristics of a
137 duplex deformation (Agate et al. 1998). Based on field observations (mesoscopic structural data
138 and stratigraphy) and on seismic profile interpretation, the S- and SW-vergent Sicilian Barracù
139 tectonic unit, overlies the carbonate platform Busambra tectonic unit along a partly buried low-
140 angle thrust surface (Fig. 1b, Catalano et al. 1998). In this region, the Rocca Busambra structure
141 appears pushed up to the surface, breaching the tectonically-overlying basinal Sicilian Units
142 (Barracù and buried units).

143

144 2.2. Lithostratigraphy and facies analysis

145 The Rocca Busambra rocks pertain to the Meso-Cenozoic Trapanese succession, where
146 shallow-water and pelagic carbonates deposited progressively (Giunta and Liguori 1975;
147 Mascle 1979; Wendt 2017). Many lithostratigraphic units, outcropping at the Rocca Busambra
148 ridge, compose the stratigraphic column (Fig. 1c, Basilone 2018). Upper Triassic-Lower
149 Liassic carbonate platform dolomites and limestone (Sciacca and Inici Formations, Marabito
150 reef limestone) are followed by Late Liassic to Late Jurassic condensed to pelagic deposits.
151 These deposits, informally named Rosso Ammonitico and known as Buccheri Formation, are
152 characterised by Fe-Mn crusts and condensed pelagites; they also fill a very dense network of
153 neptunian dykes. They are followed by Latest Jurassic-Eocene pelagic carbonates (Lattimusa,
154 Hybla and Amerillo Formations). Lower Miocene biocalcarenes, coastal glauconitic
155 calcarenites (Corleone calcarenites) and open shelf marls (San Cipirello marls) unconformably
156 cover the Meso-Cenozoic carbonates.

157 The Permian-Tortonian deposits of the Sicilian domain, largely outcropping in the Sicani
158 Mountains, are characterised by a typical deep-water carbonate succession (Mascle 1979). A
159 detailed stratigraphy and lithostratigraphy was recently revised, correlating wells and

160 outcropping data from the Sicani Mts and their buried prolongation in the subsurface of central
161 Sicily ([Basilone et al. 2016b](#)). The main bulk of the Mesozoic Sicanian rock assemblage (Fig.
162 1c) consists of deep-water Carnian-to-Lower Oligocene mudstone, carbonates and pelagic
163 marlstone (Mufara, Scillato, Barracù, Lattimusa, Hybla and Amerillo Formations), with
164 intercalations of resedimented carbonate breccias (Lower Jurassic Prizzi breccias and oolitic
165 crinoidal calcarenites), followed by Upper Oligocene-Middle Miocene clastic carbonates and
166 marls (Cardellia marls, Corleone calcarenites and San Cipirello marls).

3. Detailed observations

3.1. *Synsedimentary tectonics at Rocca Busambra* (itinerary 1, Fig. 2b)

The field trip, relatively to the itinerary 1, can be expired in a day. Starting from the Ficuzza
village (Fig. 2a, coord.: 37°53'04.62"N 13°32'35.01"E, elev.: 643m a.s.l.), this itinerary
permits to observe the naturalistic and cultural heritage of the Rocca Busambra-Corleone
region. The Ficuzza wood, dominated by oak tree, the historical Royal Palace of the Kingdom
of Sicily, and the carbonate ridge of Rocca Busambra are the main attractions of the area. The
Rocca Busambra ridge is a carbonate structural unit of the Sicilian Chain and records a variety
of tectono-sedimentary features. Stratal discontinuities, buttress unconformities, onlap and
downlap stratal terminations, gaps, condensed sequences, hardground crusts, 'in situ' breccias,
dissolution surfaces and resedimented clastic carbonates, characterise the Meso-Cenozoic
carbonate succession (Fig. 3).

The geomorphologic configuration of this region can be summarized in two different
landscape types, related to the outcropping lithologies and to the prevailing morphogenetic
processes:

183 - the carbonate highland landscape (Rocca Busambra, 1613 m a.s.l.) shows geomorphic
184 forms due to tectonics and morphoselection, such as the several paleo-surfaces, and the
185 wide, structurally controlled, scarps, hundreds of metres high;
186 - the marly-clayey hill landscape, surrounding the carbonate ridge, consists of reliefs with
187 gentle slopes, where landslides and water processes prevail. The mapped landslides,
188 mostly due to rotational creep, are both active and inactive (no recent movements in the
189 last few decades). The largest landslide bodies are more than 2 km long and 1 km wide,
190 and some tens of metres thick. Spectacular examples are mapped in the region south of
191 Monte Cardellia, where marly-clayey deposits (Cardellia marls), embedded between
192 limestone layers (“Corleone calcarenites” and Amerillo Fm), are repeatedly mobilized.
193 Consequently the “Corleone calcarenites” displays to be deformed mostly with lateral
194 spreading processes (Fig. 4, Agnesi et al. 1978; Basilone 2011). Fluvial processes
195 originated several orders of alluvial terraces (mapped along the main rivers) and
196 spectacular erosional canyons in the Corleone village area.

3.1.1. Panoramic view of the Nicolosi graben

At the km 24 of the SS118, the road crossing the Rocca Busambra ridge, we have a
beautiful view of the NW cliff of Pizzo Nicolosi (Stop 1 in Figs. 2a, b, coord.: 37°52'39.68"N
13°19'01.56"E, elev. 521 m. a.s.l.). Here a very impressive paleotectonic structure is exposed,
offering a spectacular example of graben (geological section I in Fig. 3c and Fig. 5a). The
carbonate platform sub-horizontal beds of the Inici Formation (INI) are cut by WNW-ESE
steeply dipping antithetic faults, originating depression with relative displacement of more than
50 m. The morphotectonic depression is filled by Upper Cretaceous pelagic limestone
(Amerillo Formation, AMM). These pelagites abut in buttress unconformity against the fault
planes and drape the horst eroded margins (Fig. 6, coord.: 37°51'46.98"N 13°19'22.70"E elev.:

208 929m. a.s.l., see location on Fig. 2b). Other structures, variously oriented, occur in the northern
209 side of Pizzo Nicolosi, where the tectonic depression, bounded by fault planes, originated the
210 Rocca Ramusa graben (Fig. 7, see point of observation in Fig. 2b, coord.: 37°51'57.44"N
211 13°20'19.46"E elev.: 935m. a.s.l.). This latter structure shows, only the southern flank of the
212 graben, the Jurassic and Upper Cretaceous pelagites that directly onlap and downlap the floor
213 of the depressions (Fig. 7a). They crop out, in buttress unconformity (Davies and Reynolds
214 1996), against the sub-vertical walls (Fig. 7b) and drape the horst structures (Fig. 7c).

3.1.2. The dykes of Rocca Argenteria

217 In the Rocca Argenteria quarry (Stop 2 in Figs. 2a, b, coord.: 37°51'52.18"N
218 13°19'13.17"E, elev.: 604 m. a.s.l.) we observe a dense network of neptunian dykes, cutting
219 the white peritidal limestone (Inici Formation). The latter consists of algae and mollusc-bearing
220 wackestone and oolitic packstone-grainstone organized in shallowing upward cycles, up to 400
221 m thick. Benthic foraminifera, echinoderms, rare crinoids, calcareous algae (*Cayeuxia* sp.,
222 *Thaumatoporella parvovesiculifera* (Raineri), *Paleodasycladus mediterranus* (Pia)),
223 gastropods, pelecypods, brachiopods and ammonites represent the main fossil content of the
224 Lower Liassic Inici Fm (Gemmellaro 1878; Gugenberger 1936; Arkell 1956). A regional
225 unconformity, marked by a cm-thick blackish Fe-Mn crust, characterises the top of the
226 formation, which is overlain by the *Bositra* pelagic limestone rich in ammonites (Fig. 9a).

227 The dense network of sub-vertical, oblique, and bed-parallel fractures with polyphasic fill
228 of Jurassic, Cretaceous and Miocene sediments, dissects and penetrates the topmost portion of
229 the Inici peritidal limestone (Fig. 9b, c, d). These sedimentary dykes, some of which appear
230 siphon-like structures (Masclé 2008), mutually crosscut displaying various colour. We
231 distinguished three main orientations: a) WNW-ESE trending dykes filled by mostly Jurassic
232 mudstone with ammonoids; b) NNW-SSE and N-S oriented dykes, mostly filled by planktonic

233 foraminifera-bearing wackestone of the Amerillo Formation; c) E-W and NNE-SSW trending
234 dykes, filled by glauconitic sandstones (Corleone calcarenites). Repeated re-opening of
235 individual dykes proves the tectonic control of the dyke formation (Wendt 2017).

236 Similar features may be observed in other places such as at Monte Kumeta (Mallarino et al.
237 2002; Gasparo Morticelli et al. 2017), in the Sciacca area (Rocca Porcaria, Mascle 1964), or in
238 Eastern Sicily (Truillet 1966)

240 3.1.3. Paleofaults at Piano Pilato

241 The region of Piano Pilato, located in the westernmost side of Rocca Busambra (Stop 3 in
242 Figs. 2a, b, coord.: 37°51'36.63"N 13°19'59.70"E, elev. 763 m. a.s.l.), and continuing uphill to
243 the minor reliefs of Rocca del Drago, Rocca Argenteria and Pizzo Nicolosi is characterized by
244 a Jurassic condensed pelagic facies association. It is followed by the Upper Cretaceous pelagic
245 and Lower Miocene reworked pelagic facies associations (Fig. 3a). The pelagic succession
246 covers, unconformably, the sub-horizontal beds of the Lower Jurassic peritidal limestone.

247 Several, south dipping, sub-vertical (60-80° steep) WNW-ESE oriented paleofaults (with
248 some metres of downthrown) cut the carbonate platform deposits (geological section II in Fig.
249 3c). These features, either fault planes or morphotectonic scarps (Fig. 5b), are sealed by
250 Jurassic-Cretaceous pelagites and resedimented deposits, which lie with buttress unconformity
251 against the hanging-wall scarp (Fig. 9, coord.: 37°51'27.39"N 13°20'42.88"E, elev.: 891m.
252 a.s.l.).

253 At the southern scarp of Piano Pilato, a half-graben structure bounded by E-W and WNW-
254 ESE fault planes outcrops (Figs. 3b, c, 5b). The faults cut the sub-horizontal beds of Lower
255 Liassic peritidal limestone and are sealed by Lower Miocene glauconitic reworked pelagic beds
256 that rest in buttress unconformity (geological section II in Fig. 3c); basal breccias, with angular
257 to subrounded lithoclasts of Lower Liassic peritidal limestone, embedded into Lower Miocene

258 yellowish glauconitic packstone, are present. On the southern side of the half-graben, the Lower
1
2 259 Miocene glauconitic “reworked pelagic” facies association unconformably covers the Jurassic
3
4
5 260 condensed pelagic facies association, with downlap relationships, and is conformably followed
6
7 261 by Langhian marls, which here display their maximum thickness (Fig. 3a and geological section
8
9
10 262 II in Figs. 3c).

11
12 263 In the adjacent Pirrello region, located in the central part of the ridge (Figs. 2a, b, 3), deeply
13
14 264 eroded elongated channels and WNW-ESE paleofaults and morphotectonic scarps with large
15
16
17 265 displacement, are the main tectono-sedimentary features (geological section III in Fig. 3c and
18
19 266 Fig. 5c). The channels, showing a semi-circular cross-section of 2-3 km², correspond to a
20
21
22 267 concave-upward erosional surface that is carved into the top of the Lower Liassic peritidal
23
24 268 limestone. The erosional surface is draped by Jurassic and/or Upper Cretaceous pelagites.
25
26
27 269 Lower Miocene calcarenites abut, in buttress unconformity, the sub-horizontal white peritidal
28
29 270 limestones beds along a south dipping fault scarp with a few tens of metres of downthrow
30
31
32 271 (geological section III in Fig. 3c and Fig. 5c). The top of the Lower Liassic peritidal limestones
33
34 272 is crosscut by neptunian dykes mostly filled by reddish crinoidal and *Bositra* limestone (Fig.
35
36 273 5c). Cm-thick anastomosing veins, filled with reddish or dark iron-manganese-rich carbonate
37
38
39 274 mudstone, also occur.

40
41 275

42 43 44 276 *3.2. Submarine paleo-landslides at Monte Barracù (itinerary 2, Fig. 2c)*

45
46 277 Along the state roads (SS118 and SS188c) connecting Corleone to Campofiorito it is
47
48
49 278 possible to observe spectacular examples of tectonic folds. The clastic-carbonates of the Lower
50
51 279 Miocene “Corleone calcarenites”, embedded between two marly-clayey layers (Cardellia and
52
53 280 San Cipirello marls, Fig. 1c), outcrop with variable dip, mostly sub-vertical, highlighting a
54
55
56 281 complex fold system where narrow anticline and syncline are repeatedly following one another.
57
58 282 The itinerary 2 (Figs. 2a, c), which can be expired in a day, starts from Campofiorito village
59
60
61
62
63
64
65

283 (coord.: 37°45'07.70"N 13°16'05.36"E) and develops along a motorable country road (via
1
2 284 Papa Giovanni XXIII), up to reach the next stops (stops 4, 5 in Figs. 2a, c). This road crosses a
3
4
5 285 wood, mainly dominated by pine and fir trees, making part of the larger Sicilian Regional Park.
6

7 286

9 287 *3.2.1. Panoramic view of the Barracù section*

11
12 288 The study section, located along the western side of the Monte Barracù (Figs. 2a, c), is a
13
14 289 NNW-SSE outcropping section, where the whole stratigraphic setting of the Mesozoic Sicilian
15
16 290 deep-water succession is visible (inset in Fig. 10).
17
18

19 291 From the panoramic view of the Barracù section (Stop 4 in Figs. 2a, c, coord.:
20
21 292 37°41'55.89"N 13°19'07.24"E, elev. 1063 m. a.s.l.), it is possible to observe in detail the
22
23 293 geometries, stratigraphic relationships and internal characteristics of the 15-30 m-thick white
24
25 294 calpionellid pelagic limestone of the Lattimusa Formation, interested by various
26
27 295 synsedimentary deformational structures (Fig. 10). The lower boundary of the formation is an
28
29 296 erosional truncation surface with the underlying Jurassic radiolarites and the Kimmeridgian-
30
31 297 lower Tithonian resedimented packstone-grainstone with *Saccocoma* sp. and *Protopeneroplis*
32
33 298 *striata*. On this surface, affected by stepped normal faults, the Lattimusa strata lie with onlap
34
35 299 and downlap stratal terminations or in buttress unconformity, also showing lateral pinch-out
36
37 300 (Fig. 10).
38
39
40
41
42

43 301 The Lattimusa Fm displays two main lithofacies association: the marl-dominated facies
44
45 302 (horizons a, c in Fig. 10) and the carbonate mudstone-dominated lithofacies (horizons b, d in
46
47 303 Fig. 10). Some deformed units are localized in distinct multilayer horizons (a b, d in Fig. 10).
48
49 304 They are separated from undisturbed and weakly deformed horizons (c and e in Fig. 10) by
50
51 305 unconformable or detachment surfaces. Undeformed beds drape and unconformably overlie the
52
53 306 deformed units, showing onlap and infilling geometries. Each deformed unit can be traced
54
55
56
57
58
59
60
61
62
63
64
65

1 307 laterally along the cliff for hundreds of metres, with thickness values ranging between 0.5 to 5
2 308 m, varying in morphology and degree of deformation (Fig. 10).

3
4 309 The deformed units were differentiated in two main types of slump sheets, on the basis of
5
6
7 310 the SSDSs, brittle deformations, morphology and geometry, involved lithofacies, sediment
8
9
10 311 properties and deformation mechanisms.

11
12 312 - Type 1 deformed units (horizon a in Fig. 10), involving the marl-dominated lithofacies,
13
14 313 display wedge-shaped morphology with increasing thickness towards the northern side of the
15
16
17 314 section, thinning up to disappear towards the south. The beds package shows pinch-out
18
19 315 geometry. From S to N, the deformed units display a thinner head sector mostly characterised
20
21
22 316 by extensional listric faults and a thicker toe sector characterised by thrusts and folds (Figs. 10,
23
24 317 11). The basal surface of the deformed units displays concave morphology, sometimes with
25
26
27 318 steep slope segments that rapidly flatten where they dip under the deformed masses (Fig. 10).
28
29 319 Folds, several of which are restricted to distinct slump horizons, show a wide variety of shapes
30
31
32 320 and sizes ranging between dm- to several m-thick (Figs. 10, 11a). Many folds are cylindrical
33
34 321 with straight fold axes and only some of them display box geometries in the hinge zone.
35
36 322 Asymmetrical folds, including recumbent ones and overturned beds, are diffused and are
37
38
39 323 frequently associated with small-scale thrusts that, on the whole, show preferential N-ward
40
41 324 orientations (Fig. 10). Isoclinal and recumbent folds and reverse faults/thrusts are the shortening
42
43
44 325 features that balance the stretching of the listric normal faults that mostly occur in up-slope
45
46 326 parts of the slump (S-ward); here, the missing beds slid down N-ward, thickening the toe of the
47
48
49 327 slumped bodies (Fig. 10).

50
51 328 - Type 2 deformed units, involving the carbonate mudstone-dominated lithofacies, appear as
52
53 329 elongated bodies with tabular morphology. They, while maintaining similar thickness values
54
55
56 330 along direction, display a thinning in their lateral boundaries especially towards the northern
57
58 331 side (inset in Fig. 10). Several steep scars cut the whole beds package involved in the
59
60
61
62
63
64
65

332 deformation. The scars, with planar to concave geometry, flatten downward and merge in the
333 main basal detachment surface (Figs. 10, 11c). These scars confer an overall steeped
334 morphology of the deformed units. The main internal deformational features are represented by
335 large-scale brittle and minor plastic deformations (Fig. 10). These slump sheets, appear as slides
336 that, as they moved downslope, glided on bedding surfaces (translational slump sheets). They
337 were completely decoupled from the underlying undeformed beds as result of the low viscosity
338 of the basal marl layers.

3.2.2. *Close view of the SSDSs*

339
340 Moving towards the cliff to reach the outcropping section it is possible to observe in detail
341 the SSDSs and brittle deformations characterising the slump sheets (Stop 5 in Figs. 2a, c, coord.:
342 37°44'58.29"N 13°19'23.39"E, elev. 1202 m. a.s.l.).

343
344 In the basal beds of the section, representing the Type 1 slump sheet, the main internal
345 deformations are (Fig. 11): i) contorted and disrupted beds of the thin mudstone intercalations,
346 which also display sigmoidal and concave geometry (Figs. 11a, b); ii) chaotic stratification,
347 internal stratal discordance and discontinuous beds (Fig. 11b); iii) several concave erosional
348 depressions, dm- to m- size, infilled by marl/mudstone alternations; iv) laterally discontinuous,
349 rows of ribbon-shaped deformation structures, which alternate with the small deformed
350 horizons involving the marl-dominated lithofacies comprised in the overall undeformed horizon
351 c (Figs. 10, 11c). Folds range between slightly deformed layers, defining simple and open
352 harmonic folds, to strongly contorted layers outlining tight/isoclinal disharmonic ones.
353 Sometimes, the folds include well-developed detachment surfaces and some minor sub-vertical
354 fractures (e.g., tension gashes, Fig. 11a). They pass laterally into other deformational features,
355 as contorted and disrupted beds, or undeformed intervals (Fig. 11b). Faults and fractures
356 affecting the Type 1 slump sheets are structures in the range of cm to 1 m. The throw is variable,

357 from a few centimetres to several decimetres (Figs. 10, 11a, b). In detail, we can observe: i)
358 sub-vertical extensional fractures and normal faults; ii) dm- to m-scale listric normal faults
359 dipping N-wards. They show concave geometry, dip decreases with depth, merging into sub-
360 horizontal or low-dipping detachments, and are associated with roll-over anticlines (Fig. 10);
361 iii) high angle reverse faults and thrusts, most of which show a modest displacement, are
362 associated with asymmetric folds (Figs. 10, 11a).

363 Moving up-wards, along the natural section, is possible to observe in detail the Type 2 slump
364 sheet internal deformations. The most common SSDSs (Figs. 11c, d) are: i) undulate beds with
365 lens to sigmoidal geometry; ii) truncated beds and concave erosional features; iii) few harmonic
366 isoclinal and asymmetrical folds. They are several centimetres to a few decimetres high and
367 laterally extended for a few metres (Figs. 10, 11c). The brittle deformational features are: i)
368 stepped normal faults with listric geometry affecting multiple beds (Figs. 10, 11c); ii) antithetic
369 normal faults that develop small horst and graben structures. Downwards, these faults tend to
370 merge into the main detachment surface and, towards the top, they are sealed unconformably
371 by the undeformed strata displaying onlap and infilling geometry (Figs. 10, 11d). These closely
372 spaced normal faults are, locally, associated with reverse faults and thrusts affecting the beds
373 package in the immediately downslope sector. Bulges at the toe of these faults and small
374 antithetic reverse faults are developed to accommodate the rotational component of slip that
375 generates rollover anticlines, in the hanging wall of listric faults (Figs. 10, 11c).

4. Discussion

4.1. Seismic activity caused by synsedimentary tectonic

379 In the Piano Pilato region, the several WNW-ESE oriented fault planes with small
380 displacements (geological sections I-III in Fig. 3c and Fig. 5) produced a stepped margin
381 morphostructural setting (Santantonio 1993; Basilone 2009). This interpretation is supported

382 by: i) stratigraphic buttress unconformities occurring between the faulted peritidal limestone
383 and the younger deposits, ii) subangular breccias at the fault scarps, originated from the
384 breaking up of the faulted peritidal limestone, iii) sub-vertical fault planes most of which show
385 homogeneous orientation. The faults, formed as fractures of the top of the Lower Liassic
386 peritidal limestone, were later reactivated during the Kimmeridgian, Tithonian and Late
387 Cretaceous tectonic pulses (Figs. 3, 5). They, occurring with various values of downthrown,
388 caused strong instability of the Tethyan continental margin and particularly the brittle carbonate
389 platform rocks, which could be triggered by associated earthquakes with various degrees of
390 intensity (Allen 1986; Basilone and Sulli 2016, 2018; Alsop et al. 2016).

7.2. Earthquake effects

393 The described features of the Type 1 slump sheets, recognized along the Barracù section,
394 reflect the configuration of the classical model of rotational slump sheets that locates major
395 shortening at the toe of the deformed bodies (Martinsen and Bakken 1990; Strachan and Alsop
396 2006; Ortner 2007; Alsop et al. 2017). The alternation of deformed and undeformed units
397 indicates that deformation occurred as separate events alternated with long periods of
398 undisturbed sedimentation (e.g., Sims 1975; Mastrogiacomo et al. 2012; Alsop et al. 2016). The
399 synsedimentary extensional tectonics that affected the Upper Triassic-Jurassic deep-water
400 deposits of the Barracù section caused tilt-block and instability of the seafloor through
401 fluidization processes, triggering the rotational slumps (Fig. 10). Seismic shocks, induced by
402 outside sector tectonics, like those recorded in the Busambra stepped carbonate platform
403 margin, possibly triggered the rotational slumps that are not related to the local-scale faults (see
404 Basilone 2017 for further details).

405 As the mudstone strata of the Type 2 slump sheets were partially cemented and had become
406 semi-consolidated, the gravity flow resulted in a downslope movement of the whole beds

407 package controlled by gliding-related simple shear (Ortner and Kilian 2016). The slump scars,
408 which appear to be roughly crescent-shaped (Martinez et al. 2005), have listric geometries that
409 root downwards into an underlying flat detachment surface and down-step the multilayer
410 slumps (Fig. 10, e.g., Ortner 2007; Alsop et al. 2016). The observed structures suggest that the
411 Type 2 translational slides (glides) can be included in the sediment creep model (e.g., Booth et
412 al. 1984; Silva and Booth 1984; Shillington et al. 2012; Ortner and Kilian 2016). To explain
413 the translational glides of the upper portion of the section (Fig. 10), the aforementioned outside
414 sector earthquakes could produce instability of the sea-floor through thixotropy of marls.

7.3. Geoconservation

417 Many of the modern landslides, developing both onshore and offshore, are triggered by
418 earthquakes (Agnesi et al, 2005; Paparo et al, 2017). Wideworld examples reflect strong
419 similarities with the studied features, both in geometries and trigger mechanisms (Fig. 12a).
420 The Mesozoic Busambra and Barracù structures reflect strong similarities with modern
421 continental margins, where stepped normal faults and submarine landslides are highly diffused
422 (Fig. 12b).

423 This comparison suits the principle of actualism (“the present is the key of the past”, Leyll,
424 1830-1833) and represent an important turning point that enhance the geological interest of the
425 two sites. Furthermore, the described structures and the related processes help to identify the
426 geological province where faults and landslides can develop and how can be observed their
427 effects on the landscape.

428 Considering both the good exposition of the sedimentary and structural features related to
429 paleo-earthquakes and their geological interest, the conservation of this heritage is a necessity
430 not only as scientific objects, but also as important educational resources and/or attractive
431 geotourism products. Thus, promoting the institution of these geosites may have a coupled

432 fruition. The naturalistic-cultural purpose is justified by the spectacular landscape characterised
433 by variable geomorphological setting, occurrence of ancient woods and the architectural-
434 historical significance of the Royal Palace of Ficuzza. Furthermore, the geological heritage may
435 be used for the observation of the described features both for geotourists and for educational
436 training. The latter assumes a crucial role also considering the disaster due to recent earthquakes
437 in Central and Southern Italy (Figs. 12c-d, Belice, Amatrice, Irpinia earthquakes). An
438 educational training, made on the field, may have a key role to understand the described
439 phenomena and their effects on the landscape. It may be a useful tool for the prevention of the
440 geohazard. In this view, this paper and the suggested field trip are also addressed to an
441 institutional audience consisting both of politicians and public administrators.

443 **Conclusions**

444 The Rocca Busambra and Monte Barracù, located in the western Sicani Mountains, near
445 Corleone (Palermo), are adjacent carbonate reliefs where causes and effects of Mesozoic
446 earthquakes are spectacularly exposed.

447 They consist of Mesozoic shallow-water to condensed-pelagic and deep-water carbonate
448 successions, respectively. In the western side of Rocca Busambra (Piano Pilato and Nicolosi
449 regions), the several WNW-ESE oriented paleofaults produce horst and graben and steeped
450 margin tectonic setting. These faults, cutting the Lower Liassic carbonate platform deposits,
451 are draped by the younger pelagites with buttress unconformity. In the Barracù section, several
452 tectonic features, including synsedimentary faults and seismically-induced submarine slump
453 sheets, characterised the outcrop. Some of these gravitational deformations have been
454 interpreted as rotational and translational slides.

455 Therefore, the features described along the itineraries 1 and 2, and relative stops, allow us to
456 propose a field trip to recognise causes and landscape effects of earthquakes. In this view, as

1 457 suggested by the IUGS (International Union of Geological Science) and by the UNESCO,
2 458 geosite proposition for the two areas is recommended to promote geotourism and to preserve
3
4
5 459 the cultural and geological heritage (geoconservation).
6

7 460 The recent earthquakes occurred in Central and Southern Italy require more attention to these
8
9
10 461 problematics. An educational training, as that proposed in this field trip, could represent a useful
11
12 462 tool to understand earthquakes activity and landscape products. Moreover, the focus
13
14 463 highlighted by this paper could be of specific interests for public administrators, whose rapid
15
16
17 464 and skilled action is necessary for the prevention and reduction of geohazards.
18

19 465
20

21
22 466 *Aknowledgments:* Funding for research was provided by CARG (F_607 Corleone fondi della
23 467 Legge 438/95 finanziamenti '96, F_608 Caccamo fondi della Legge 67/88). We are grateful to
24 468 an anonymous reviewer and to the Editor Kevin Page for the useful comments to the
25 469 manuscript.
26

470 **References**

- 1
2 471 Agate M, Basilone L, Catalano R, Franchino A, Merlini S, Sulli A (1998) Monte Barracù: Deformazione interna
3 472 delle Unità Sicane nell'area tra Corleone e Monte Colomba. In: Catalano R, Lo Cicero G (eds.), La Sicilia, un
4 473 laboratorio naturale nel Mediterraneo. Strutture, Mari, Risorse e Rischi. Guida alle Escursioni del 79°
5 474 Congresso Nazionale della Società Geologica Italiana – La Sicilia Occidentale, 1:79–88. Mondello (Palermo,
6 475 Italia), 21-23 settembre 1998.
- 7 476 Agate M, Basilone L, Di Maggio C, Contino A, Pierini S, Catalano R (2017) Quaternary marine and continental
8 477 unconformity-bounded stratigraphic units of the NW Sicily coastal belt. *Journal of Maps* 13 (2):425–437.
9 478 <http://dx.doi.org/10.1080/17445647.2017.1314229>
- 10 479 Agnesi V, Macaluso T, Monteleone S, Pipitone G (1978) Espansioni laterali (lateral spreads) nella Sicilia
11 480 Occidentale. *Geol. Applicata e Idrogeologia*, 13:319–326.
- 12 481 Agnesi V, Camarda M, Conoscenti C, Di Maggio C, Serena Diliberto I, Madonia P, Rotigliano E (2005) A
13 482 multidisciplinary approach to the evaluation of the mechanism that triggered the Cerda landslide (Sicily, Italy).
14 483 *Geomorphology* 65:101–116. doi:10.1016/j.geomorph.2004.08.003
- 15 484 Allen JRL (1986) Earthquake magnitude-frequency, epicentral distance, and soft-sediment deformation in
16 485 sedimentary basins. *Sedimentary Geology* 46 (1-2):67–75, doi:10.1016/0037-0738(86)90006-0.
- 17 486 Alsop GI, Marco S, Weinberger R, Levi T (2016) Sedimentary and structural controls on seismogenic slumping
18 487 within mass transport deposits from the Dead Sea Basin: *Sedimentary Geology* 344:71–90,
19 488 doi:10.1016/j.sedgeo.2016.02.019.
- 20 489 Alsop GI, Marco S, Levi T, Weinberger R (2017) Fold and thrust systems in Mass Transport Deposits: *Journal of*
21 490 *Structural Geology* 94:98–115, doi:10.1016/j.jsg.2016.11.008.
- 22 491 Amodio Morelli L, Bonardi G, Colonna V, Dietrich D, Giunta G, Ippolito F, Liguori V, Lorenzoni S, Paglionico
23 492 A, Perrone V, Piccarreta G, Russo M, Scandone P, Zanettin Lorenzoni E, Zuppetta A (1976) L'arco Calabro-
24 493 Peloritano nell'orogene Appenninico-Maghrebide. *Mem Soc Geol Ital* 17:1–60
- 25 494 Arkell WJ (1956) *Jurassic geology of the world*. Oliver & Boyd, Edinburgh
- 26 495 Basilone L (2009) Mesozoic tectono-sedimentary evolution of the Rocca Busambra (western Sicily). *Facies*
27 496 55:115–135, doi: 10.1007/s10347-008-0156-2
- 28 497 Basilone L (2011) Geological Map of the Rocca Busambra-Corleone region (western Sicily, Italy): explanatory
29 498 notes. *Italian Journal of Geoscience (Boll. Soc. Geol. It.)* 130:42–60, doi: 10.3301/IJG.2010.17
- 30 499 Basilone L (2017) Seismogenic rotational slumps and translational glides in pelagic deep-water carbonates. Upper
31 500 Tithonian-Berriasian of Southern Tethyan margin (W Sicily, Italy). *Sedimentary Geology* 356:1–14.
32 501 <http://dx.doi.org/10.1016/j.sedgeo.2017.04.009>
- 33 502 Basilone L (2018) *Lithostratigraphy of Sicily*. Unipa Springer Series, p. 1-349. Springer International Publishing
34 503 AG. <https://doi.org/10.1007/978-3-319-73942-7>
- 35 504 Basilone L, Di Maggio C (2016) Geology of Monte Gallo (Palermo Mts, NW Sicily). *Journal of Map* 12 (5):1072–
36 505 1083. doi: 10.1080/17445647.2015.1124716
- 37 506 Basilone L, Sulli A (2016) A facies distribution model controlled by a tectonically inherited sea bottom topography
38 507 in the carbonate rimmed shelf of the Upper Tithonian-Valanginian Southern Tethyan continental margin (NW
39 508 Sicily, Italy). *Sedimentary Geology* 342:91–105. doi: 10.1016/j.sedgeo.2016.06.013
- 40 509 Basilone L, Sulli A (2018) Basin analysis in the Southern Tethyan margin: Facies sequences, stratal pattern and
41 510 subsidence history highlight extension-to-inversion processes in the Cretaceous Panormide carbonate platform
42 511 (NW Sicily) *Sedimentary Geology* 363: 235–251 doi:10.1016/j.sedgeo.2017.11.013
- 43 512 Basilone L, Lena G, Gasparo-Morticelli M (2014) Synsedimentary tectonic, soft-sediment deformation and
44 513 volcanism in the rifted Tethyan margin from the Upper Triassic-Middle Jurassic deep-water carbonates in
45 514 Central Sicily. *Sedimentary Geology* 308:63–79. doi: 10.1016/j.sedgeo.2014.05.002
- 46 515 Basilone L, Sulli A, Gasparo Morticelli M (2016a) The relationships between soft-sediment deformation structures
47 516 and synsedimentary extensional tectonics in Upper Triassic deep-water carbonate succession (Southern
48 517 Tethyan rifted continental margin - Central Sicily). *Sedimentary Geology* 344:310–322.
49 518 doi:10.1016/j.sedgeo.2016.01.010
- 50 519 Basilone L, Frixia A, Trinciante E, Valenti V (2016b) Permian-Cenozoic deep-water carbonate rocks of the
51 520 Southern Tethyan Domain. The case of Central Sicily. *Italian Journal of Geoscience (Boll Soc Geol It)*
52 521 135:171–198. doi:10.3301/IJG.2015.07
- 53 522 Bergerat FO, Collin P-Y, Ganzhorn A-C, Baudin F, Galbrun B, Rouget I, Schnyder J (2011) Instability structures,
54 523 synsedimentary faults and turbidites, witnesses of a Liassic seismotectonic activity in the Dauphiné Zone
55 524 (French Alps): A case example in the Lower Pliensbachian at Saint-Michel-en-Beaumont: *Journal of*
56 525 *Geodynamics* 51 (5), 344–357. doi: 10.1016/j.jog.2010.10.003.
- 57 526 Bertok C, Martire L (2009) Sedimentation, fracturing and sliding on a pelagic plateau margin: the Middle Jurassic
58 527 to Lower Cretaceous succession of Rocca Busambra (Western Sicily, Italy). *Sedimentology* 56: 1016–1040.

- 528 Bigi G, Cosentino D, Parotto M, Sartori R, Scandone P (1990) Structural Model of Italy: Geodynamic Project:
 1 529 Consiglio Nazionale delle Ricerche, S.EL.CA, scale 1:500,000
- 2 530 Bolt BA (1993) Earthquakes. W.H. Freeman, 331 pp.
- 3 531 Booth J, Silva A, Jordan S (1984) Slope-stability analysis and creep susceptibility of Quaternary sediments on the
 4 532 northeastern United States continental slope. In: Denness B (Ed.), Seabed Mechanics. Springer, Netherlands,
 5 533 pp. 65–75.
- 6 534 Bourrouilh R (1998) Synsedimentary tectonics, mud-mounds and sea-level changes on a Palaeozoic carbonate
 7 535 platform margin: a Devonian Montagne Noire example (France). *Sedimentary Geology* 118:95–118.
- 8 536 Catalano R, Franchino A, Merlini S, Sulli A, Agate M, Basilone L (1998) Materiali per la Comprensione
 9 537 dell'Assetto Profondo della Sicilia Centro-Occidentale. In: Catalano R, Lo Cicero G (Eds.) Guida alle
 10 538 escursioni. La Sicilia occidentale vol I: 175-185, 79° Congresso della Soc Geol It, Palermo.
- 11 539 Catalano R, Franchino A, Merlini S, Sulli A (2000) A crustal section from North Algeria to the Ionian ocean
 12 540 (Central Mediterranean). *Memorie della Società Geologica Italiana*, 55:71–85.
- 13 541 Catalano R, Gatti V, Avellone G, Basilone L, Frixia A, Ruspi R, Sulli A (2008) Subsurface geometries in central
 14 542 Sicily FTB as a premise for hydrocarbon exploration. 70th European Association of Geoscientists and
 15 543 Engineers Conference and Exhibition 2008: Leveraging Technology. Incorporating SPE EUROPEC
 16 544 2008, 1:69–73. ISBN: 978-160560474-9
- 17 545 Catalano R, Avellone G, Basilone L, Sulli A (2010) Note illustrative della Carta Geologica d'Italia alla scala
 18 546 1:50.000, foglio n. 607 "Corleone", 240 pp. Istituto Superiore per la Protezione e la Ricerca Ambientale,
 19 547 Servizio Geologico d'Italia; Roma. ISBN 978-88-240-2972-8
 20 548 http://www.isprambiente.gov.it/MEDIA/carg/607_CORLEONE/Foglio.html
- 21 549 Catalano R, Avellone G, Basilone L, Gasparo-Morticelli M, Lo Cicero G (2011) Note illustrative della carta
 22 550 geologica d'Italia alla scala 1: 50.000 foglio 608 Caccamo. 224 pp. Istituto Superiore per la Protezione e la
 23 551 Ricerca Ambientale, Servizio Geologico d'Italia; Roma. ISBN 978-88-240-2973-5
 24 552 http://www.isprambiente.gov.it/MEDIA/carg/608_CACCAMO/Foglio.html
- 25 553 Davis GH, Reynolds SJ (1996) Structural geology. John Wiley & Sons, New York.
- 26 554 Di Maggio C, Agate M, Contino A, Basilone L, Catalano R (2009) Unconformity-bounded stratigraphic units of
 27 555 Quaternary deposits mapped for the CARG Project in Northern and Western Sicily [Unità a limiti inconformi
 28 556 utilizzate per la cartografia dei depositi quaternari nei fogli CARG della Sicilia nord-occidentale]. *Alpine and
 29 557 Mediterranean Quaternary* 22 (2):345–364. Open Access
- 30 558 Eder FW, Patzak M (2004) Geoparks-geological attractions: A tool for public education, recreation and sustainable
 31 559 economic development. *Episodes* 27 (3), 162–164.
- 32 560 Festa A, Dilek Y, Gawlick H-J, Missoni S (2014) Mass-transport deposits, olistostromes and soft-sediment
 33 561 deformation in modern and ancient continental margins, and associated natural hazards. *Marine Geology* 356:
 34 562 1–4. doi: 10.1016/j.margeo.2014.09.001
- 35 563 Finetti IR, Lentini F, Carbone S, Del Ben A, Di Stefano A, Forlin E, Guarnieri P, Pipan M, Prizzon A (2005)
 36 564 Geological outline of Sicily and Lithospheric Tectono-Dynamics of its Tyrrhenian Margin from new CROP
 37 565 Seismic Data. Crop Project: Deep Seismic Exploration of the Central Mediterranean and Central Italy. Edited
 38 566 by IR Finetti, 2005 Elsevier B.V.
- 39 567 Gamboa D, Alves T, Cartwright J, Terrinha P (2010) MTD distribution on a 'passive' continental margin: The
 40 568 Espirito Santo Basin (SE Brazil) during the Palaeogene. *Marine and Petroleum Geology* 27:1311–1324.
 41 569 doi:10.1016/j.marpetgeo.2010.05.008
- 42 570 Garcia-Tortosa FJ, Alfaro P, Gibert L, Scott G (2011) Seismically induced slump on an extremely gentle slope
 43 571 (<1) of the Pleistocene Tecopa paleolake (California). *Geology* 39: 1055–1058. doi:10.1130/G32218.1
- 44 572 Garcia-Rodriguez MJ, Malpica JA (2010) Assesment of earthquake-triggered landslide susceptibility in El
 45 573 Salvador based on an artificial Neural Network model. *Natural Hazards Earth System Science*, 10: 1–9
 46 574 doi:10.5194/nhess-10-1-2010
- 47 575 Gasparo Morticelli M, Valenti V, Catalano R, Sulli A, Agate M, Avellone G, Albanese C, Basilone L, Gugliotta
 48 576 C (2015) Deep controls on foreland basin system evolution along the Sicilian fold and thrust belt. *Bulletin de
 49 577 la Societé géologique de France* 186: 273–290. doi:10.2113/gssgfbull.186.4-5.273
- 50 578 Gasparo Morticelli M, Avellone G, Sulli A, Agate M, Basilone L, Catalano R, Pierini S (2017) Mountain building
 51 579 in NW Sicily from the superimposition of subsequent thrusting and folding events during Neogene: structural
 52 580 setting and tectonic evolution of the Kumeta and Pizzuta ridges. *Journal of Maps* 13: 276–290.
 53 581 doi:10.1080/17445647.2017.1300546
- 54 582 Gemmellaro GG (1878) Sui fossili del calcare cristallino delle Montagne del Casale e di Bellolampo nella
 55 583 Provincia di Palermo, pp. 1872–1882 Palermo
- 56 584 Giunta G, Liguori V (1975) Considerazioni sul significato ambientale e sul ruolo paleotettonico della Rocca
 57 585 Busambra (Sicilia). *Boll Soc Nat Napoli* 84:45–49
- 58 586 Grandjacquet C, Mascle G (1978) The Structure of the Ionian Sea, Sicily, and Calabria-Lucania. In: AEM
 59 587 Nairn, WH Kaner, FG Stehli (eds) *The ocean basins and margins*, pp. 257–329. Springer, Boston, MA
- 60 587

- 588 https://doi.org/10.1007/978-1-4684-3039-4_5
- 1 589 Gugenberger O (1936) I cefalopodi del Lias Inferiore della Montagna del Casale in provincia di Palermo (Sicilia).
2 590 *Palaeontogr Ital* 37:135–213
- 3 591 Keefer DK (2002) Investigating landslides caused by earthquakes—a historical review. *Surveys in Geophysics*,
4 592 23:473–510
- 5 593 Kopf AJ, Stegmann S, Garziglia S, Henry P, Dennielou B, Haas S, Weber K-C (2016) Soft sediment deformation
6 594 in the shallow submarine slope off Nice (France) as a result of a variably charged Pliocene aquifer and mass
7 595 wasting processes. *Sedimentary Geology* 344:290–309. doi:10.1016/j.sedgeo.2016.05.014
- 8 596 Leeder MR (1987) Sediment deformation structures and the palaeotectonic analysis of sedimentary basins, with a
9 597 case-study from the Carboniferous of northern England. In: Jones ME, Preston RMF (Eds.), *Deformation of*
10 598 *Sediments and Sedimentary Rocks: Journal of the Geological Society of London, Special Publication*, 29:137–
11 599 146.
- 12 600 Leeder MR (2010) *Sedimentology and Sedimentary Basins. From Turbulence to Tectonics*. Wiley-Blackwell.
- 13 601 Lowe DR (1976) Subaqueous liquefied and fluidized sediment flows and their deposits. *Sedimentology* 23:285–
14 602 308.
- 15 603 Lyell C (1830-1833) *Principles of geology, being an attempt to explain the former changes of the Earth's surface,*
16 604 *by reference to causes now in operation*. Vol. 1-2-3, London, John Murray.
- 17 605 Lunina O., Gladkov AS (2016) Soft-sediment deformation structures induced by strong earthquakes in southern
18 606 Siberia and their paleoseismic significance. *Sedimentary Geology* 344: 5–19.
19 607 doi:10.1016/j.sedgeo.2016.02.014
- 20 608 Malamud BD, Turcotte DL, Guzzetti F, Reichenbach P (2004) Landslides, earthquakes, and erosion. *Earth and*
21 609 *Planetary Science Letters*, 229:45-59
- 22 610 Mallarino G, Goldstein RH, Di Stefano P (2002) New approach for quantifying water depth applied to the enigma
23 611 of drowning of carbonate platforms. *Geology* 30: 783–786. doi:10.1130/0091-
24 612 7613(2002)030<0783:NAFQWD>2.0.CO;2
- 25 613 Maltman AJ, 1984. On the term ‘soft-sediment deformation’. *Journal of Structural Geology* 6: 589–592.
- 26 614 Martinez JF, Cartwright J, Hall B (2005) 3D seismic interpretation of slump complexes: examples from the
27 615 continental margin of Israel. *Basin Research* 17:83–108.
- 28 616 Martinsen OJ (1994) Mass Movements. In: A. Maltman (Ed), *The Geological Deformation of Sediments*.
29 617 Chapman & Hall, London, pp. 127–165.
- 30 618 Martinsen OJ, Bakken B (1990) Extensional and compressional zones in slumps and slides in the Namurian of
31 619 County Claire, Eire. *Journal of the Geological Society of London* 147:153-164.
- 32 620 Martire L, Montagnino D (2002) Stop 10 Rocca Argenteria: a complex network of Jurassic to Miocene neptunian
33 621 dykes. In: Santantonio M (ed) 6th international symposium on the Jurassic system. *General Field Trip*
34 622 *Guidebook*, Palermo, pp 87–91
- 35 623 Mascle G (1964) Les couches des passages du Jurassique au Cretaceé de la serie de Sciacca (monts Sicani, Sicile).
36 624 C.R.S.S. Soc Geol Fr 199–200 (Paris).
- 37 625 Mascle G (1970) Geological sketch of western Sicily. In Alvarez W, *Geology and history of Sicily*.
- 38 626 Mascle G (1973) Geologie sur la structure de Rocca Busambra (Sicile occidentale): mise en évidence d'une
39 627 tectonique antécénomaniennne. *CR Academia Science Paris* 276: 265–267.
- 40 628 Mascle G (1979) Etude géologique des Monts Sicani. *Rivista Italiana di Paleontologia e Stratigrafia* 16:1–430.
- 41 629 Mascle G (2008) *Les roches, mémoire du temps*. EDP Sciences, 287 pp. ISBN: 978-2-7598-0044-5
- 42 630 Mastalerz K, Wojewoda J (1993) Alluvial-fan sedimentation along an active strike-slip fault: Plio-Pleistocene Pre-
43 631 Kaczawa fan, SW Poland. In: Marzo, M., Puigdefabregas, C. (Eds.), *Alluvial Sedimentation*. International
44 632 Association of Sedimentologists (IAS) Special Publication 17, 293–304.
- 45 633 Mastrogiacomo G, Moretti M, Owen G, Spalluto L (2012) Tectonic triggering of slump sheets in the Upper
46 634 Cretaceous carbonate succession of the Porto Selvaggio area (Salento peninsula, southern Italy):
47 635 Synsedimentary tectonics in the Apulian Carbonate Platform. *Sedimentary Geology* 269-270:15–27.
48 636 doi:10.1016/j.sedgeo.2012.05.001
- 49 637 Miall AD (2016) The valuation of unconformities. *Earth-Science Reviews* 163:22–71.
50 638 doi:10.1016/j.earscirev.2016.09.011
- 51 639 Mocco P, Kristek J, Gális M (2014) *The Finite-Difference Modelling of Earthquake Motions: Waves and*
52 640 *Ruptures*. Cambridge University Press, 383 pp.
- 53 641 Monaco C, Tortorici L, Catalano S (2000) Tectonic escape in the Sicanian mountains (western Sicily). *Memorie*
54 642 *Società Geologica Italiana* 55:17–25
- 55 643 Moretti M, Alfaro P, Owen G (2016) The environmental significance of soft-sediment deformation structures: key
56 644 signatures for sedimentary and tectonic processes. *Sedim Geol* 344:1–4. doi:10.1016/j.sedgeo.2016.10.002
- 57 645 Nishimura T (2017) Triggering of volcanic eruptions by large earthquakes, *Geophysical Research*
58 646 *Letters*, 44:7750–7756, doi: 10.1002/2017GL074579.
- 59 647 Obermeier SF (1996) Using liquefaction-induced features for paleoseismic analysis. In: McCalpin, J.P. (Ed.),

- 648 Paleoseismology. *International Geophysical Research* 62:331–396.
- 1 649 Ogniben L (1960) Note illustrative dello schema geologico della Sicilia Nord-Orientale. *Rivista Mineraria*
2 650 *Siciliana* 64-65:183–212, Palermo.
- 3 651 Oldow JS, Channell JET, Catalano R, D'Argenio B (1990) Contemporaneous thrusting and large-scale rotations
4 652 in the Western Sicilian fold and thrust belt. *Tectonics* 9:661–681
- 5 653 Ortner H (2007) Styles of soft-sediment deformation on top of a growing fold system in the Gosau Group at
6 654 Muttekopf, Northern Calcareous Alps, Austria: slumping versus tectonic deformation. *Sedimentary Geology*
7 655 196:99–118.
- 8 656 Ortner H, Kilian S (2016) Sediment creep on slopes in pelagic limestone: Upper Jurassic of Northern Calcareous
9 657 Alps, Austria. *Sedimentary Geology* 344:350–363. doi:10.1016/j.sedgeo.2016.03.013
- 10 658 Owen G, Moretti M (2011) Identifying triggers for liquefaction-induced soft-sediment deformation in sands.
11 659 *Sedimentary Geology* 235:141–147.
- 12 660 Owen G, Moretti M, Alfaro P (2011) Recognising triggers for soft-sediment deformation: Current understanding
13 661 and future directions. *Sedimentary Geology* 235:133–140.
- 14 662 Paparo AM, Armigliato A, Pagnoni G, Zaniboni F, Tinti S (2017) Earthquake-triggered landslides along the
15 663 Hyblean-Malta Escarpment (off Augusta, eastern Sicily, Italy) - assessment of the related tsunamigenic
16 664 potential. *Advances in Geosciences* 44:1–8. doi:10.5194/adgeo-44-1-2017
- 17 665 Posamentier H, Martinsen OJ (2011) The character and genesis of submarine mass-transport deposits: insights
18 666 from outcrop and 3D seismic data, in: Shipp C, Weimer P, Posamentier H (Eds.), *Mass-transport deposits in*
19 667 *deepwater settings*. *SEPM Special Publication* 96:7–38.
- 20 668 ProGEO (2011) Conserving our shared geoheritage – a protocol on geoconservation principles, sustainable site
21 669 use, management, fieldwork, fossil and mineral collecting. [http://www.progeo.se/progeoprotocol-definitions-](http://www.progeo.se/progeoprotocol-definitions-20110915.pdf)
22 670 [20110915.pdf](http://www.progeo.se/progeoprotocol-definitions-20110915.pdf) (13 October 2015)
- 23 671 Roure F, Howell DG, Muller C, Moretti I (1990) Late Cenozoic subduction complex of Sicily. *Journal of Structural*
24 672 *Geology* 12 (2):259–266.
- 25 673 Santantonio M (1993) Facies associations and evolution of pelagic carbonate platform/basin systems: examples
26 674 from the Italian Jurassic. *Sedimentology* 40:1039–1067. doi:10.1111/j.1365-3091.1993.tb01379.x
- 27 675 Seilacher A (1969) Fault-graded beds interpreted as seismites. *Sedimentology* 13:155–159.
- 28 676 Seth A, Sarkar S, Bose PK (1990) Synsedimentary seismic activity in an immature passive margin basin (Lower
29 677 Member of the Katrol Formation, Upper Jurassic, Kutch, India). *Sedimentary Geology* 68:279–291.
- 30 678 Shillington DJ, Seeber L, Sorlien CC, Steckler MS, Kurt H, Dondurur D, Çifçi G, İmren C, Cormier M-H, McHugh
31 679 CMG, Gürçay S, Poyraz D, Okay S, Atgın O, Diebold JB (2012) Evidence for widespread creep on the flanks
32 680 of the Sea of Marmara transform basin from marine geophysical data. *Geology* 40 (5): 439–442.
- 33 681 Silva AJ, Booth JS (1984) Creep behaviour of submarine sediments. *Geo-Marine Letters* 4 (3–4): 215–219.
- 34 682 Sims JD (1975) Determining earthquake recurrence intervals from deformational structures in young lacustrine
35 683 sediments. *Tectonophysics* 29: 141–152.
- 36 684 Strachan JS, Alsop GI (2006) Slump folds as estimators of palaeoslope: a case study from the Fisherstreet Slump
37 685 of County Clare, Ireland. *Basin Research* 18: 451–470.
- 38 686 Strasser A, Heitzmann P, Jordan P, Stapfer A, Stürm B, Vogel A, Weidmann M (1995) Géo-topes et la protection
39 687 des objets géologiques en Suisse: un rapport stratégique – Fribourg: Groupe suisse pour la protection des
40 688 géotopes. 27p.
- 41 689 Strasser M, Moore GF, Kimura G, Kopf AJ, Underwood MB, Guo J, Scream EJ (2011) Slumping and mass
42 690 transport deposition in the Nankai fore arc: evidence from IODP drilling and 3-D reflection seismic data.
43 691 *Geochemistry, Geophysics, Geosystems* 12 (5): Q0AD13. <http://dx.doi.org/10.1029/2010GC003431>.
- 44 692 Truillet R (1966) Existence de filons sédimentaires homogènes et granoclassés dans les environs de Taormina
45 693 (monts Peloritains-Sicile). *C. R. Som. Soc. Geol. France* 9:354–359 Paris
- 46 694 Üner S, Alırız MG, Özsayın E, Selçuk AS, Karabıykoğlu M (2017) Earthquake Induced Sedimentary Structures
47 695 (Seismites): Geoconservation and Promotion as Geological Heritage (Lake Van-Turkey). *Geoheritage* 9:133–
48 696 139. doi:10.1007/s12371-016-0186-z
- 49 697 Vai GB, Martini P (Eds) (2001) *Anatomy of an orogen: the Apennines and adjacent Mediterranean basins*.
50 698 Blackwell Academic Publisher, 433 pp.
- 51 699 Van Loon AJT, Pisarska-Jamroży M (2014) Sedimentological evidence of Pleistocene earthquakes in NW Poland
52 700 induced by glacio-isostatic rebound. *Sedimentary Geology* 300:1–10. doi:10.1016/j.sedgeo.2013.11.006
- 53 701 Wendt J (1965) Synsedimentaire Bruchtektonik im Jura Westsiziens. *N Jb Geol Paläontol Mh* 5:286–311
- 54 702 Wendt J (2017) A unique fossil record from neptunian sills: the world's most extreme example of stratigraphic
55 703 condensation (Jurassic, western Sicily). *Acta Geologica Polonica* 67:163–199. doi:10.1515/agp-2017-0015
- 56 704 Walter TR, Amelung F (2007) Volcanic eruptions following $M \geq 9$ megathrust earthquakes: Implications for the
57 705 Sumatra-Andaman volcanoes. *Geology*, 35: 539–542, doi:10.1130/G23429A.
- 58 706 Wimbledon WAP (1997) Geosites – a new conservation initiative. *Episodes*, 19: 87–88.
- 59
60
61
62
63
64
65

707 **Captions**

1
2 708 Fig. 1. Simplified geological map of the Central-Western Sicily (a). Inside, the tectonic map of
3
4
5 709 the Central Mediterranean (after [Catalano et al., 2000](#)); legend: 1. Corsica-Sardinian
6
7 710 units; 2. Calabrian Arc and Kabylia units; 3. Maghrebian-Sicilian-Southern Apennine
8
9
10 711 FTB and deformed foreland; 4. Foreland and mildly folded foreland; 5. Areas with
11
12 712 superimposed extension; 6. Plio-Quaternary volcanites. (b) Geological cross-section
13
14 713 showing the tectonic relationships among the outcropping Barracù (Sicanian) and Rocca
15
16 714 Busambra (Trapanese) tectonic units (after [Catalano et al. 1998](#); [Basilone 2011](#)). (c)
17
18
19 715 Chronostratigraphic scheme showing the lithostratigraphic units of the Trapanese and
20
21
22 716 Sicanian successions (after [Basilone 2018](#)).

23
24 717 Fig. 2. Map of the proposed field itineraries and relative stops.

25
26 718 Fig. 3. Measured stratigraphic sections along the Rocca Busambra ridge (a). See Fig. 1c for the
27
28
29 719 legend. In the inset map are reported the location of the study stratigraphic sections and
30
31 720 the reconstructed tectonic profiles (I-III). Structural map of the Rocca Busambra ridge
32
33
34 721 that displays different trending faults and their age (b). NNE-SSW tectonic profiles
35
36 722 showing the depositional setting of the different regions along the Rocca Busambra ridge
37
38
39 723 (c).

40
41 724 Fig. 4. Panoramic view showing landslides, where blocks of various dimension of the
42
43
44 725 “Corleone calcarenites” are moved by lateral spreading processes.

45
46 726 Fig. 5. (a) Graben structures at Pizzo Nicolosi. The Upper Cretaceous pelagic limestone (*AMM*,
47
48 727 coloured in green) abut, in buttress unconformity, the sub-horizontal Lower Liassic
49
50
51 728 peritidal limestone beds (*INI*) and the *Bositra* limestone (*BCH₁*) along WNW-ESE faults,
52
53 729 thus forming depressions with relative downthrown of more than 50 m (Rocca Ramusa
54
55
56 730 and Pizzo Nicolosi grabens) and draping the horst erosional margins. (b) Panoramic view
57
58 731 of the southern slope of Piano Pilato showing stepped faults and paleoscarps; *INI* lower
59
60
61
62
63
64
65

732 Jurassic peritidal limestone; *J* Jurassic deposits. (c) The Pirrello region is characterized
1
2 733 by scalloped margin features, showing unconformable relationships between the infilling
3
4 734 Upper Cretaceous pelagic limestone (coloured in light green, *AMM*), Lower Miocene
5
6 735 glauconitic grainstone (coloured in yellow *CCR*) and the faulted Lower Jurassic platform
7
8 736 beds (*INI*). Panoramic picture shows neptunian dykes (in white), E-W and ENE-WSW
9
10
11
12 737 paleofault trends (coloured in red).
13

14 738 Fig. 6. View of the angular contact in buttress unconformity between the sub-vertical Upper
15
16
17 739 Cretaceous pelagic beds (*AMM*) and the faulted Lower Jurassic platform beds (*INI*); fault
18
19 740 plane is coloured in red (Pizzo Nicolosi, westernmost side of Rocca Busambra).
20

21 741 Fig. 7. Close-up of the “Rocca Ramusa graben” filled by the Upper Cretaceous pelagic
22
23
24 742 limestones (*AMM*, in green) that onlap the peritidal limestones on the floor of the graben
25
26
27 743 (a) and abut, in buttress unconformity, the sub-horizontal beds of *INI* in the southern flank
28
29 744 of the structure (b); fault plane is the area coloured in red. Angular relationships between
30
31 745 *AMM* and *INI* along the horst (c).
32
33

34 746 Fig. 8. a) Blackish Fe-Mn crust (hardground) capping the top of the white peritidal limestone
35
36 747 (Inici Formation, *INI*) and followed by the *Bositra* limestone (*BCH*₁) at Rocca Drago (see
37
38
39 748 Fig. 2b for location). Detail of the Fe-Mn crust showing pinnacle structures (b). Topmost
40
41 749 portion of the Lower Liassic white peritidal limestone of the Inici Formation (*INI*) at
42
43 750 Rocca Argenteria (see Fig. 2b for location) characterised by reddish neptunian dykes
44
45
46 751 subparallel and orthogonal to the stratification (c). Close view of the network of neptunian
47
48
49 752 dyke filled by reddish *Bositra* limestone where angular fragments of the host rock, eroded
50
51 753 by the sides of the fracture, are merged (d-e). f) Paleokarst cavities carved in the white
52
53 754 peritidal limestone (*INI*) and filled by Upper Cretaceous reddish pelagic limestone
54
55
56 755 (*AMM*) and by the Lower Miocene green-yellowish glauconitic calcarenites (*CCR*).
57
58
59
60
61
62
63
64
65

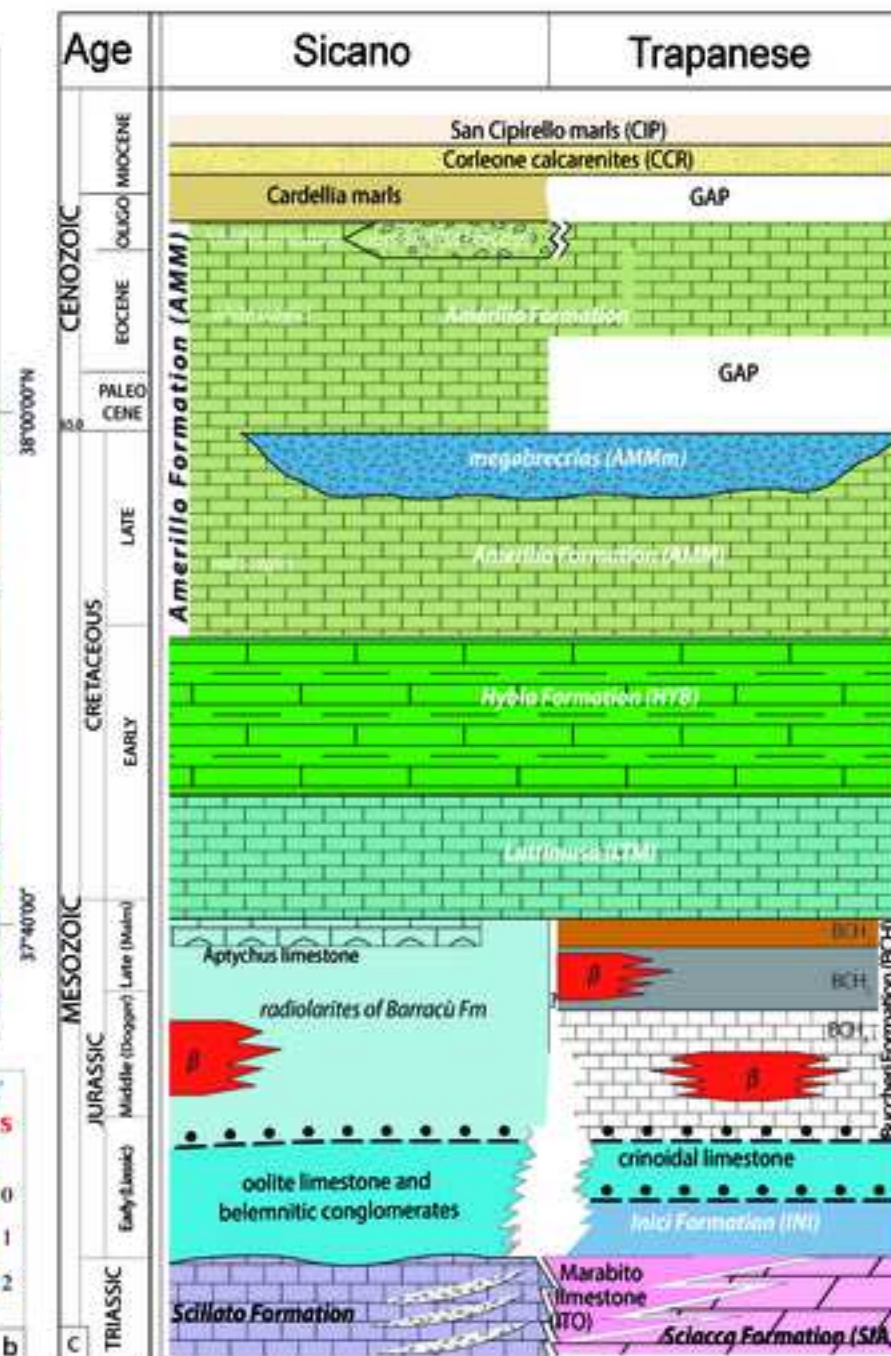
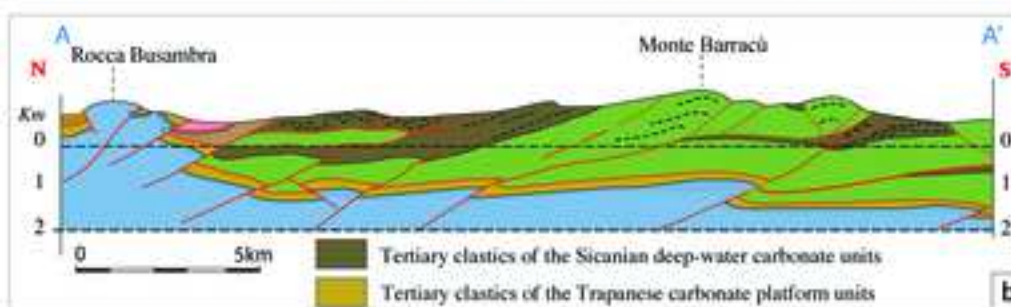
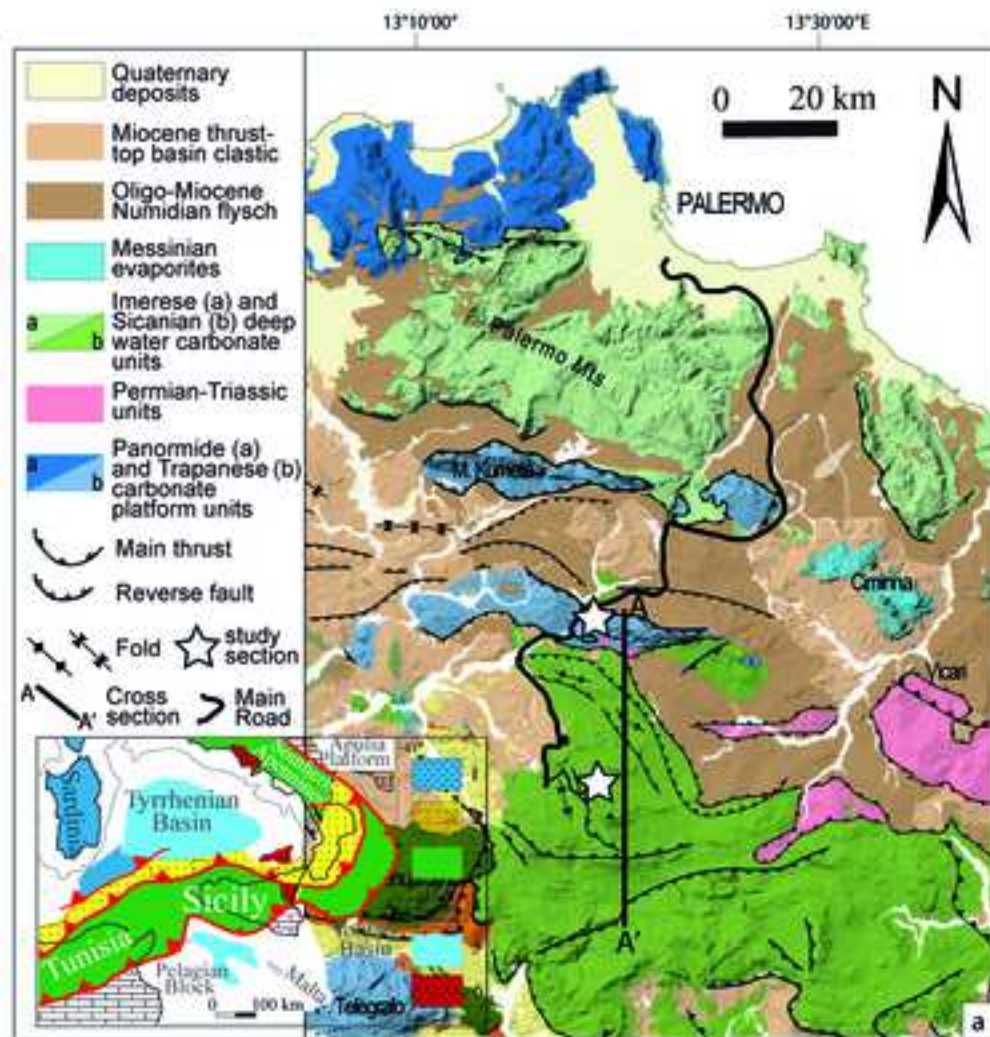
756 Fig. 9. Field evidence and sketch of the fault plane that dissected the Lower Liassic peritidal
1 limestone of the Inici Fm (1) and *Bositra* limestone (2) in the Piano Pilato region. The
2 757 limestone of the Inici Fm (1) and *Bositra* limestone (2) in the Piano Pilato region. The
3
4 758 Upper Jurassic *Saccocoma* limestone (3) lie with a buttress unconformity against the
5
6 hanging-wall scarp of the fault plane and in downlap on the sub-horizontal *Bositra*
7 759 limestone of the footwall block (after Basilone 2009).
8
9 760 limestone of the footwall block (after Basilone 2009).
10

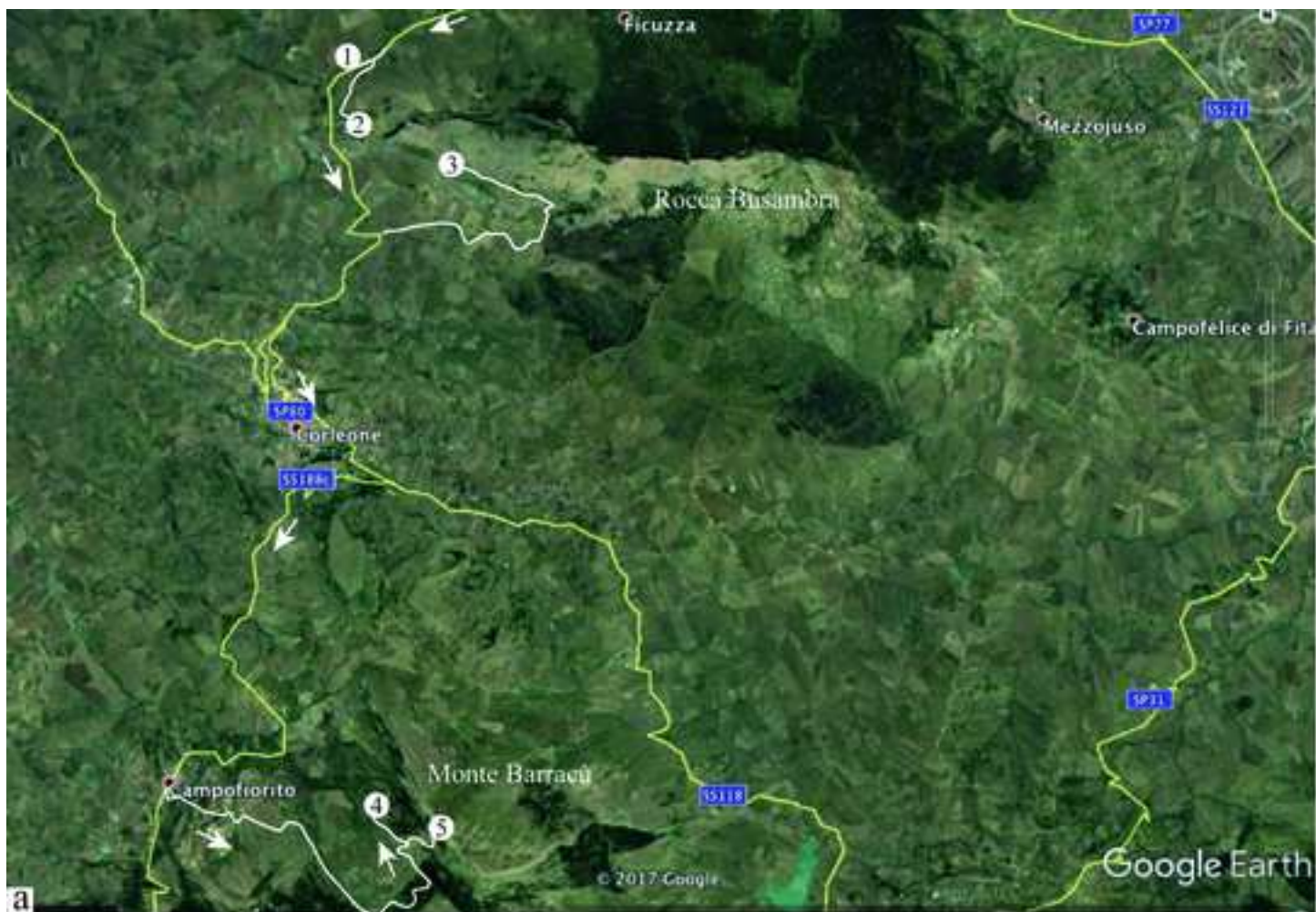
11
12 761 Fig. 10. Panoramic view and line drawing of the upper Tithonian-Berriasian deformed
13
14 762 calpionellid limestone of the Lattimusa Fm., showing the differentiated slump sheets,
15
16 SSDSs and brittle deformations. Inside, panoramic view of the western side of Monte
17 763 Barracù, showing the whole Triassic-Lower Oligocene Sicilian carbonate succession.
18
19 764 The upper Tithonian-Berriasian calpionellid limestone, towards the North, displays an
20
21 undeformed thin-bedded succession passing southwards to a deformed succession and
22 765 thinning in its southernmost portion (after Basilone 2017).
23
24 766
25
26 767
27
28

29 768 Fig. 11. Field photographs and line drawings of the SSDSs recognised in the slump sheets of
30
31 769 Monte Barracù: a) fault and fold deformation restricted to a distinct slump horizon;
32
33 various structures, including disrupted, discontinued and cross-laminated beds are
34 770 observed in the limestone interlayered with marls. On the right, an ENE-WSW oriented
35
36 771 symmetric anticlinal fold is affected by sub-vertical tension gashes and sedimentary
37
38 injections of marls. NNW-thrust beds and NNW-dipping extensional faults also occur;
39 772 b) contorted and disrupted beds with oblique laminations and internal discordance. The
40
41 773 deformation structures are concentrated along a detachment surface parallel to the
42
43 bedding (bold line) that was the original marl level (grey). Normal spineless faults are
44 774 also present; c) listric normal faults and scar cutting the whole beds package of the B and
45
46 775 D horizons (see Fig. 10). Faults flatten downward merging into the main detachment
47
48 776 surfaces, which locally are dissected by reverse faults; d) SSDSs in the deformed horizon
49
50
51 777
52
53 778
54
55
56 779
57
58
59
60
61
62
63
64
65

780 B, including internal stratal discordance with downlap and toplap stratal termination,
1
2 781 truncated features and infilling geometry.
3

4
5 782 Fig. 12. Examples of landslides induced by earthquakes: a) aerial view of the landslide triggered
6
7 783 by the Santa Tecla earthquake (2001) in El Salvador (after [García-Rodríguez and Malpica](#)
8
9 784 [2010](#)); b) 3D bathymetric model from North-eastern Sicily offshore. The Multibeam data
10
11 785 show earthquake-induced submarine landslides in a modern active continental margin.
12
13 786 The main scarp affects the shelf edge, at -125 m, and the continental slope, while the
14
15 787 landslide deposits lie at the toe located at about 450-500 m in an intra-slope basin; c)
16
17 788 landslide related to the fault with 1 m of downthrow observable at the top of the hill and
18
19 789 formed during the Amatrice earthquake (2016) in Central Italy (Sibillini Mts., Apennines,
20
21 ©Google); d) rockfalls in the Peistocene calcarenites of the Agrigento Fm, triggered by
22
23 790 the Belice earthquake (1968) in Sicily (Montevago – AG, photo S. Monteleone).
24
25 791
26
27 792
28
29
30
31
32
33
34
35
36
37
38
39
40
41
42
43
44
45
46
47
48
49
50
51
52
53
54
55
56
57
58
59
60
61
62
63
64
65





a

Itinerary 1

Itinerary 2



b



c

